Toxicology Letters 288 (2018) 119–128

Contents lists available at ScienceDirect

Toxicology Letters

journal homepage: www.elsevier.com/locate/toxlet

Factor X activating *Atractaspis* snake venoms and the relative coagulotoxicity neutralising efficacy of African antivenoms

Brice Oulion[a,1], James S. Dobson[a,1], Christina N. Zdenek[a,1], Kevin Arbuckle[b], Callum Lister[a], Francisco C.P. Coimbra[a], Bianca op den Brouw[a], Jordan Debono[a], Aymeric Rogalski[a], Aude Violette[c], Rudy Fourmy[c], Nathaniel Frank[d], Bryan G. Fry[a,*]

[a] *Venom Evolution Lab, School of Biological Sciences, University of Queensland, St Lucia, QLD 4072, Australia*
[b] *Department of Biosciences, College of Science, Swansea University, Swansea SA2 8PP, UK*
[c] *Alphabiotoxine Laboratory sprl, Barberie 15, 7911 Montroeul-au-bois, Belgium*
[d] *Mtoxins, 1111 Washington Ave, Oshkosh, WI 54901, USA*

ARTICLE INFO

Keywords:
Venom
Antivenom
Coagulopathy
Thrombin
Fibrinogen
Snake

ABSTRACT

Atractaspis snake species are enigmatic in their natural history, and venom effects are correspondingly poorly described. Clinical reports are scarce but bites have been described as causing severe hypertension, profound local tissue damage leading to amputation, and deaths are on record. Clinical descriptions have largely concentrated upon tissue effects, and research efforts have focused upon the blood-pressure affecting sarafotoxins. However, coagulation disturbances suggestive of procoagulant functions have been reported in some clinical cases, yet this aspect has been uninvestigated. We used a suite of assays to investigate the coagulotoxic effects of venoms from six different *Atractaspis* specimens from central Africa. The procoagulant function of factor X activation was revealed, as was the pseudo-procoagulant function of direct cleavage of fibrinogen into weak clots. The relative neutralization efficacy of South African Antivenom Producer's antivenoms on *Atractaspis* venoms was boomslang > > > polyvalent > saw-scaled viper. While the boomslang antivenom was the most effective on *Atractaspis* venoms, the ability to neutralize the most potent *Atractaspis* species in this study was up to 4–6 times less effective than boomslang antivenom neutralizes boomslang venom. Therefore, while these results suggest cross-reactivity of boomslang antivenom with the unexpectedly potent coagulotoxic effects of *Atractaspis* venoms, a considerable amount of this rare antivenom may be needed. This report thus reveals potent venom actions upon blood coagulation that may lead to severe clinical effects with limited management strategies.

1. Introduction

Species in the *Atractaspis* genus within the Lamprophiidae snake family are nocturnal burrowing venomous snakes (Spawls and Branch, 1995). This genus represents the third independent evolution of front-fangs within snakes (Fry et al., 2015). Their fangs erect on a horizontal plane rather than on a vertical plane like in viperids, resulting in descriptive common names including switchblade snakes and stiletto snakes. Bites are characterized by strong, local pain accompanied by swelling and localized tissue necrosis (amputation resulting in some survivors), coagulation disturbances including elevated partial thromboplastin time and decreased prothrombin index, rapid and severe hypertension, and deaths have been recorded (Coppola and Hogan, 1992; Kochva, 1998; Kurnik et al., 1999; Lee et al., 1986; Leisewitz et al., 2004; Tilbury and Verster, 2016).

Despite their evolutionary novelty and documented severe envenomation effects, their venom is underinvestigated relative to the intensive efforts on elapid and viperid snake venoms. Work to-date has largely focused on the endothelin-type peptides called sarafotoxins which are responsible for the dramatic rise in blood pressure observed clinically (Abd-Elsalam, 2011; Atkins et al., 1995; Borgheresi et al., 2001; Goyffon, 1994; Ismail et al., 2007; Kawanabe and Nauli, 2011; Kolb, 1991; Mahjoub et al., 2015; Malaquin et al., 2016; Nakajima et al., 1989; Nayler et al., 1989; Patocka et al., 2004; Takasaki et al., 1992; Tilbury and Verster, 2016; Warrell et al., 1976). The only other characterized toxin type from *Atractaspis* venom has been a hemorrhagic metalloprotease (Ovadia, 1987). Transcriptome sequencing has shown that toxin types present in the venom include peptides (three

* Corresponding author.
E-mail address: bgfry@uq.edu.au (B.G. Fry).
[1] Contributed equally.

https://doi.org/10.1016/j.toxlet.2018.02.020
Received 24 December 2017; Received in revised form 8 February 2018; Accepted 13 February 2018
Available online 17 February 2018
0378-4274/

finger, AVIT, beta-defensin, c-type lectin, cystatin, sarafotoxin, waprin), non-enzymatic proteins (CRiSP, lipocalin, nerve growth factor) and enzymes (acetylcholinesterase, kallikrein-type serine protease, metalloprotease, phospholipase A_2) (Terrat et al., 2013).

In snake venoms, procoagulant toxin types include metalloproteases (Casewell et al., 2015; Debono et al., 2017; Rogalski et al., 2017), kallikrein-type serine proteases (Vaiyapuri et al., 2015) and mutant forms of the blood factors FXa and FVa which are specifically expressed in venom glands (Cipriani et al., 2017; Earl et al., 2015; Lister et al., 2017; Trabi et al., 2015). Procoagulant functions produce endogenous thrombin by Factor V activation (Vaiyapuri et al., 2015), Factor VII activation (Cipriani et al., 2017), Factor X activation (Casewell et al., 2015; Vaiyapuri et al., 2015) and prothrombin activation (Casewell et al., 2015; Rogalski et al., 2017; Trabi et al., 2015). The endogenous thrombin in turn cleaves fibrinogen to form normal, well cross-linked, and strong clots. Procoagulant functions may be accompanied by synergistic functions such as Factor XIII activation by kallikrein-type serine proteases to further cross-link the fibrin mesh (Vaiyapuri et al., 2015), and plasmin inhibition by kunitz peptides to prevent plasmin from degrading the clots (Eng et al., 2015). This aids in prey subjugation through the rapid induction of stroke, while conversely in human victims the venom is diluted into a much larger blood volume resulting in defibrinogenation, with death due to internal bleeding such as cerebral hemorrhage (Debono et al., 2017; Herrera et al., 2012; Jackson et al., 2016).

Anticoagulant functions in snake venoms occur in two forms: pseudo-procoagulant functions in which a part of the clotting cascade is catalyzed to produce unstable, weak clots which are readily broken down; and true anticoagulant functions in which clot formation is directly impeded. The pseudo-procoagulant action involves the atypical cleavage of fibrinogen by apotypic kallikrein-type serine proteases (Vaiyapuri et al., 2015) to form poorly cross-linked clots with short half-lives, leading to a net anticoagulant state (Fry et al., 2015; Hutton and Warrell, 1993). In contrast, true anticoagulant kallikrein-type serine proteases or metalloproteases cleave fibrinogen in a destructive, non-clotting manner that not only directly depletes the amount of fibrinogen available for clot formation, but the fibrinogen degradation products may also be bound by thrombin and thus also reduce the amount of thrombin available for clot formation (Casewell et al., 2015; Vaiyapuri et al., 2015).

Both pseudo-procoagulant and anticoagulant functions may be accompanied by a myriad of synergistic functions including: alpha-2 antiplasmin blockage by kallikrein-type serine proteases (Vaiyapuri et al., 2015); antithromboplastic effects to prevent the formation of the prothrombinase complex by Group II PLA_2 (Sunagar et al., 2015b); Factor V denaturation by kallikrein-type serine proteases (Vaiyapuri et al., 2015); inhibition of the enzymatic activity of Factor VIIa and the Factor VIIa/tissue factor complex by three finger toxins (Utkin et al., 2015); Factor Xa inhibition by kunitz peptides (Eng et al., 2015); plasminogen activation by kallikrein-type serine proteases (Vaiyapuri et al., 2015); plasminogen activator release from endothelial cells by vascular permeability by kallikrein-type serine proteases and metalloproteases (Casewell et al., 2015; Vaiyapuri et al., 2015); platelet inhibition through receptor binding by disintegrins (separately and coupled to metalloproteases); Group I and Group II PLA_2, lectins and three finger toxins (Arlinghaus et al., 2015; Casewell et al., 2015; Sunagar et al., 2015a,b; Utkin et al., 2015); protein C activation by kallikrein-type serine proteases (Vaiyapuri et al., 2015); thrombin inhibition by kunitz peptides (Eng et al., 2015); and blood vessel wall degradation by kallikrein-type serine proteases and metalloproteases (Casewell et al., 2015; Vaiyapuri et al., 2015). Both pseudo-procoagulant and anticoagulant functions promote haemorrhagic shock, whether in prey or human victims (Boyer et al., 2015).

Although coagulotoxic effects are suggested by the scarce clinical reports of *Atractaspis* envenomations, no laboratory studies have been undertaken to elucidate these effects. This study aims to fill these knowledge gaps by subjecting the venoms to a battery of assays to determine the nature and potency of effects upon the clotting cascade. We examined the three broad mechanisms of coagulotoxicity: procoagulant functions leading to thrombin production; pseudo-procoagulant functions upon fibrinogen with net anticoagulant outcomes; or true anticoagulant functions upon fibrinogen.

2. Materials and methods

2.1. Venoms examined

This study examined six *Atractaspis* specimens from five African countries in order to ascertain the nature and potency of coagulotoxic functions and the relative inhibition by available antivenoms. Specimen codes, species designation (as concluded by venom suppliers) and confirmed geographic origin were as follows: SP01 *A. irregularis* Congo; SP02 *A. bibroni* Tanzania; SP03 *A. atterima* Ghana; SP04 *A. fallax* Kenya; SP05 *A. bibroni* Tanzania; and SP06 *A. irregularis* Cameroon.

2.2. Coagulation analyses and relative antivenom efficacy

Coagulation analyses and relative antivenom efficacy studies were conducted as previously described by us (Debono et al., 2017; Lister et al., 2017; Rogalski et al., 2017). Coagulation analyses were performed on a Stago STA-R Max® automated coagulation analyser (Stago, Asnières sur Seine, France) using Stago Analyser software v0.00.04 (Stago, Asnières sur Seine, France). All experiments were conducted in triplicate, with plasma and venom being replaced every 15–30 min to minimise enzyme degradation.

To check the quality of the plasma (Australian Red Cross research approval #16-04QLD-10; 44 Musk Street, Kelvin Grove, Queensland 4059), positive and negative controls were conducted and compared to pre-established plasma clotting parameters in the presence and absence of an activator (49–51 sec (s) and 526–586 s respectively). The positive control was conducted by performing a standardised activated Partial Thromboplastin Time (aPTT) test (Stago Cat#T1203 TriniCLOT APTT HS). In this test, 50 µl Kaolin (STA C.K.Prest standard kit, Stago Cat#00597), a coagulation activator, was added to 50 µl plasma and incubated for 120 s. Then, 50 µl $CaCl_2$ (0.025 M, Stago Cat#00367) was added, and time until clot formation was measured. As a negative control, test conditions in the absence of venom were replicated: 50 µl buffer solution (30 µl 50% deionised H_2O/50% glycerol in 270 µl Owren-Koller (OK) buffer) was added to 50 µl $CaCl_2$, 50 µl phospholipid and 25 µl OK buffer, and then incubated for 120 s at 37 °C. 75 µl plasma was then added and clotting time measured. Both controls were run in triplicate before commencing any venom analyses.

In order to determine clotting times effected by the addition of varying venom concentrations, venom working stock solution was manually diluted with Owren Koller (OK) Buffer (Stago Cat# 00360) as appropriate in order to perform 10-point dilution series (µg/ml: 20, 10, 5, 2.5, 1.33, 0.66, 0.4, 0.2, 0.1, and 0.05). 50 µl of $CaCl_2$ with 50 µl phospholipid (cephalin prepared from rabbit cerebral tissue from STA C.K Prest standard kit, Stago Cat# 00597, solubilised in OK Buffer) were added to 50 µl of the diluted venom. An additional 25 µl of OK Buffer was added to the cuvette and incubated for 120 s at 37 °C before adding 75 µl human plasma (total volume 250 µl/cuvette). Time until clot formation was then immediately monitored by the automated analyser.

In order to test for co-factor dependence of the venoms, the aforementioned coagulation analyses were run both with and without $CaCl_2$ and/or phospholipid. The experimental protocol was identical, with the exception that 50 µl OK Buffer was added as a substitute for the removed co-factor to ensure consistency in final test volumes (250 µl).

The relative efficacy of polyvalent and monovalent antivenoms were investigated in this study. The previously measured whole plasma clotting times for each venom were used as a baseline comparison for

the effects of three antivenoms: SAVP boomslang antivenom Lot M03852, SAVP polyvalent antivenom Lot L01146, and SAVP saw-scaled viper antivenom Lot 2147. For antivenom testing, all test conditions replicated that of the coagulation analyses, with the exception that 25 µl of antivenom working solution (50 µl reconstituted antivenom in 950 µl OK buffer) was used in place of 25 µl of OK Buffer: 50 µl venom, 50 µl calcium, 50 µl phospholipid, 25 µl antivenom, 120 s incubation time, 75 µl plasma. Time until clot formation was then immediately measured.

Coagulation times (sec) for each of the venoms and antivenoms were graphed using Prism 7.0 software (GraphPad Software Inc, La Jolla, CA, USA) to produce concentration response curves. Calculation of EC_{50} (concentration of venom at which 50% of the effect is observed) values for the venom and antivenom concentration curves for each dataset were performed using Prism 7.0 software. Data are expressed as mean ± SD. After EC_{50}s were calculated, the relative antivenom efficacy as indicated by x-fold shift in the clotting curve was calculated using the formula:

$x = ((abc)/(def)) - 1$

a = antivenom EC_{50} x-axis

b = antivenom EC_{50} y-axis

c = antivenom starting clotting time

d = venom EC_{50} x-axis

e = venom EC_{50} y-axis

f = venom starting clotting time.

Values ‘c’ and ‘f’ account for the initial shift in clotting time observed for the highest venom concentration (20 µg/ml) when comparing conditions in the presence vs. the absence of antivenom. Subtraction of ‘1’ transforms the calculated ratio into a value representing the x-fold shift of the clotting curves following antivenom addition. For example, if there is no shift of the antivenom curve compared to venom curve (ie. the numerator divided by the denominator), then the parenthetical value would equal one, and one minus one would result in a zero-shift value for antivenom efficacy.

2.3. Calibrated automated thromography (CAT)

Calibrated automated thrombography studies were conducted as previously described by us (Lister et al., 2017). Thrombin generation was measured by a Calibrated Automated Thrombogram (CAT, Stago), using the method previously described by Hemker (Hemker, 2005; Hemker et al., 2003, 2002). The following was pipetted into a 96-well round-bottom microtiter plate (Thermo Fisher Scientific, Waltham, Massachusetts, USA): a starting volume of 80 µl of pre-warmed human plasma (37 °C), 10 µl of venom, and 10 µl of phospholipid. The plate was then inserted into a Thermo Fisher Fluoroskan fluorometer (Thermo Labsystem, Helsinki, Finland). The default 10-min incubation step was removed so as to capture the initial thrombin formation. Prior to starting, dispensing lines were washed and then primed with pre-warmed 2.5 mmol/l fluorogenic substrate in 5 mmol/l CaCl2 (FluCa-Kit; Diagnostica Stago). The test was then automatically initiated by dispensing 20 µl of the fluorogenic substrate into each well and run at 37 °C for 60-min, with readings automatically taken every 20 s. For each test, venom was added to an enzymatic buffer (150 mM NaCl & 50 mM Tris–HCL, pH 7.4) and manually pipetted into the wells for final concentrations of 0.083 µg/ml. Tests were performed in triplicate for each experiment with three calibrators per half plate. Calibrators adjusted for any internal filter effects and eliminated any variation in plasmas. For the calibrator assays, phospholipid and a venom trigger was substituted with a thrombin-α2-macroglobulin complex solution of a known concentration (thrombin calibrator, Stago, US). For each thrombin generation measurement, the following parameters were recorded by the Thrombinoscope software (Maastricht, The Netherlands): the endogenous thrombin potential (ETP), represented by the activity of free thrombin multiplied by the time it remains active in the plasma (area under the curve); maximum concentration of thrombin (peak); and lag-time (time to start). The RAW data was then converted by the Thrombinoscope software into thrombin activity (nM) corresponding to the calibrator (Hemker, 2005; Hemker et al., 2003, 2002).

2.4. Zymogen activation: Factor X and prothrombin

To determine the relative rate of Factor X activation by the venom samples, the following were added into each well using a 384-well plate (black, Lot#1171125, nunc™ Thermo Scientific, Rochester, NY, USA) and performed in triplicate per venom: 10 µl of 0.001 µg/µl venom, 10 µl of 0.01 µg/µl human Factor X zymogen (Haematologic Technologies Inc. HCP-0050), and 10 µl each of $CaCl_2$ (0.025 M, Stago Catalog # 00367) and phospholipid (cephalin prepared from rabbit cerebral tissue adapted from STA C.K Prest standard kit, Stago Catalog # 00597), solubilised in 5 ml of OK Buffer (STA Owren Koller Buffer (Stago Cat# 00360)). Immediately thereafter, 60 µl of quenched fluorescent substrate was automatically dispensed per well (total volume of 100 µl in the well; 20 µl/5 ml OK buffer) using the following substrate: ES011 (Boc-Val-Pro-Arg-AMC. Boc: *t*-Butyloxycarbonyl; 7-Amino-4-methylcoumarin) (Lot #: NZY08, www.rndsystems.com). The hydrolysis reaction was monitored via fluorescence at 320/405 nm (excitation/emission). The amount of fluorescence was measured every 10 s for a total of 400 min. The machine was programmed to shake the plate for three sec before each reading to maintain homogeneity in the wells, and the plate was warmed in the machine to 37 °C to mimic the human body. Human Factor Xa enzyme (0.01 µg/µl) (7.5 mg/ml HCXA -OO60 – R & D systems) was used as positive control to ensure functionality of the substrate. Human Factor X (0.01 µg/µl) was used as a negative control to ensure it did not directly cleave the substrate without the presence of venom.

2.5. Thromboelastography

Clot strength assays were conducted using a Thromboelastograph (TEG5000) using 3.2% citrated human plasma or 4 mg/ml human fibrinogen. 72 µl of 0.025 M $CaCl_2$ to reverse citration (Stago catalog# 00367), 72 µl phospholipid from the STA CK Prest (Stago catolog# 00597), 20 µl of µl OK buffer, and 7 µl 1 µg/µl crude venom were added before 189 µl plasma or fibrinogen were added and the test immediately started. Results were obtained for 30 min. If no clot was formed, 7 ul of thrombin from the Stago Liquid Fib Kit (Stago catalog# 00673) was added in order to perform a Claussian test (Clauss, 1957)

2.6. Cleavage of fibrinogen

Fibrinogen cleavage studies were conducted as previously described by us (Dobson et al., 2017; Koludarov et al., 2017). 1 mm 12% SDS-PAGE gels were prepared using the following recipe for the resolving gel layer: 3.3 ml deionised H_2O, 2.5 ml 1.5 M Tris–HCl buffer pH 8.8 (Tris – Sigma-Aldrich, St. Louis, MO, USA; HCl – Univar, Wilnecote, UK), 100 µl 10% SDS (Sigma-Aldrich, St. Louis, MO, USA), 4 ml 30% acrylamide mix (Bio-Rad, Hercules, CA, USA), 100 µl 10% APS (Bio-Rad, Hercules, CA, USA), 4 µl TEMED (Bio-Rad, Hercules, CA, USA); and stacking gel layer: 1.4 ml deionised H_2O, 250 µl 0.5 M Tris–HCl buffer pH 6.8, 20 µl 10% SDS (Sigma-Aldrich, St. Louis, MO, USA), 330 ml 30% acrylamide mix (Bio-Rad, Hercules, CA, USA), 20 µl 10% APS (Bio-Rad, Hercules, CA, USA), 2 µl TEMED (Bio-Rad, Hercules, CA, USA). 10× gel running buffer was prepared using the following recipe: 250 mM Tris (Sigma-Aldrich, St. Louis, MO, USA), 1.92 M glycine (MP Biomedicals), 1% SDS (Sigma-Aldrich, St. Louis, MO, USA), pH 8.3.

Human fibrinogen was reconstituted to a concentration of 2 mg/ml

in isotonic saline solution, flash-frozen in liquid nitrogen and stored at −80 °C until use. Freeze-dried venom was reconstituted in deionised H_2O and concentrations were measured using a Thermo Scientific™ NanoDrop 2000. Assay concentrations were a 1:10 ratio of venom:fibrinogen. The following was conducted in triplicate for each venom: Five "secondary" aliquots containing 10 µl buffer (5 µl of 4× Laemmli sample buffer (Bio-Rad, Hercules, CA, USA), 5 µl deionised H_2O, 100 mM DTT (Sigma-Aldrich, St. Louis, MO, USA)) were prepared. A "primary" aliquot of fibrinogen (volume/concentration as per the above) was warmed to 37 °C in an incubator. 10 µl was removed from the primary aliquot ("0 min incubation" fibrinogen control) and added to a secondary aliquot, pipette mixed, and boiled at 100 °C for 4 min. 4 µg (dry weight) of venom was then added to the primary aliquot of fibrinogen (amounting to 0.1 mg/ml of venom and 1 mg/ml of fibrinogen in 40 µl total volume), pipette mixed, and immediately returned to the incubator. At each incubation time period (1 min, 5 min, 20 min, and 60 min), 10 µl was taken from the primary aliquot, added to a secondary aliquot, pipette mixed, and boiled at 100 °C for 4 min. The secondary aliquots were then loaded into the gels and run in 1× gel running buffer at room temperature for 20 min at 90 V (Mini Protean3 power-pack from Bio-Rad, Hercules, CA, USA) and then 120 V until the dye front neared the bottom of the gel. Gels were stained with colloidal coomassie brilliant blue G250 (34% methanol (VWR Chemicals, Tingalpa, QLD, Australia), 3% orthophosphoric acid (Merck, Darmstadt, Germany), 170 g/l ammonium sulfate (Bio-Rad, Hercules, CA, USA), 1 g/l coomassie blue G250 (Bio-Rad, Hercules, CA, USA)), and destained in deionised H_2O.

To quantify the band intensities in the gels, scanned gel images were uploaded to ImageJ (Version 1.4.3.67, NIH, 2006). Gel images were converted to black and white and adjusted for brightness and contrast. Using the rectangular tool, control bands were selected and defined as the first lane. Subsequent bands comprising of venom treatments with incubations of 1, 10, 20, 30, 40, 50 and 60 min were defined as lanes 2–8. Selected bands were then plotted, and each peak was isolated using the line-drawing function by drawing vertical lines down from the center of each trough. Using the wand function, band-intensity values were automatically produced by clicking on isolated peaks. These values were then exported to Excel, where the degradation of fibrinogen chains was calculated as proportions of the control.

2.7. Cleavage of fluorescent substrates

Fluorescent substrate cleavage studies were conducted as previously described by us (Cipriani et al., 2017; Debono et al., 2017; Dobson et al., 2017; Koludarov et al., 2017). A working stock solution of freeze-dried venom was reconstituted in a buffer containing 50% deionised H_2O/50% glycerol (> 99.9%, Sigma) at a 1:1 ratio to preserve enzymatic activity and reduce enzyme degradation with the final venom concentration of 0.1 mg/ml, and then stored at −20 °C. For assessing the PLA_2 activity a fluorescence substrate assay (EnzChek® Phospholipase A_2 Assay Kit, ThermoFisher Scientific). A working stock solution of freeze dried venom was reconstituted in a buffer containing 50% deionised H_2O/50% glycerol (99.9%, Sigma) at a 1:1 ratio to preserve enzymatic activity and reduce enzyme degradation with the final venom concentration of 0.1 mg/ml, and then stored at −20 °C. Venom solution (0.1 µg in dry venom weight) was brought up to 12.5 µl in PLA_2 reaction buffer (250 mM Tris–HCL, 500 mM NaCl, 5 mM $CaCl_2$, pH 8.9) and plated out in triplicates on a 384 well plate. Triplicates were measured by adding 12.5 µl quenched 1 mM EnzChek® Phospholipase A_2 substrate per well (total volume 25 µl/well) over 100 cycles at an excitation of 485 nm and emission of 520 nm, using a Fluoroskan Ascent (ThermoFisher Scientific). The negative control consisted of PLA_2 reaction buffer and substrate only.

For testing on RDES substrates (Fluorogenic Peptide Substrate, R & D systems Cat#s ES001, ES002, ES005 AND ES0011, Minneapolis, Minnesota), 10ul of 0.01 µg/µl venom stock was plated in triplicate on a 384-well black plate and measured by adding 90 µl quenched fluorescent substrate per well. The substrate concentration was 10 µl of each substrate stock solution dissolved into 4.990 ml of enzyme buffer (150 mM NaCl and 50 mM Tri-HCl pH 7.4). Fluorescence was monitored over 400 min or until activity ceased. Excitation was at 320 nm and emission was at 405 nm for substrates ES001, ES002 and ES005. Excitation was at 390 nm and emission was at 460 nm for substrate ES011. The machine was programmed to shake the plate for three sec before each reading to maintain homogeneity in the wells.

2.8. Statistical analyses

All variables were measured in triplicate for each sample and the mean values for each sample were used to test for Pearson's correlations between antivenom efficacy, clotting time, CAT, TEG, factor X activation, activity on Substrate 2, and cleavage of each fibrinogen chain. We note that some may argue for a non-parameteric equivalent such as Spearman's rank correlation due to the small sample sizes ($N = 6$ for all correlations except for antivenom vs clotting time which is $N = 4$), but variables passed a Shapiro-Wilks test of normality (unsurprisingly due to the small samples and low power of this test) and, more importantly, we were interested in the actual values of the variables rather than their ranks. Nevertheless, we note that Spearman's rank correlations give qualitatively similar or identical results to the Pearson's correlations we report herein.

3. Results

3.1. Coagulation analyses and relative antivenom efficacy

To evaluate pro- or anticoagulation activities, assessment was carried out on an automated viscosity-based (mechanical) detection system analyzer (Stago STA-R Max) that measures clotting times with a maximum reading time of 999 s – the analyzer's limit. There was significant variation between samples in the ability to clot plasma, with times to clot (in sec) at the maximum venom concentration tested (20 µg/ml) being: SP01 (19.1 ± 0.20 s), SP02 (100 ± 4.76 s), SP03 (537.13 ± 16.06 s), SP04 (50.03 ± 1.59 s), SP05 (23.77 ± 0.49 s), and SP06 (379.50 ± 16.96 s) (Fig. 1). Only SP03 did not significantly differ relative to the spontaneous clotting time of this batch of re-calcified plasma (556.33 ± 29.92 s). The actions were shown to be calcium-dependent, with the complete abolition of activity in the absence of calcium. The relative presence of phospholipid was also a driving factor but to a much less extent, with the venoms clotting slower in the absence of phospholipid by a ratio of: 1.9 (SP01), 1.7 (SP02), 1.7 (SP04), and 1.8 (SP05).

In addition to clotting ability varying significantly between the specimens, antivenom efficacy also varied moderately between samples (Fig. 1). Testing on SP01 revealed that the boomslang antivenom (8.55 ± 1.2 times shift in clotting curve) was much more effective than the polyvalent (3.2 ± 0.09 times shift in clotting curve) or saw-scaled viper (1.84 ± 0.01 times shift in clotting curve). Therefore, for the other species boomslang antivenom was tested, with relative clotting curve shifts of: SP02 (21.78 ± 0.89 times shift in clotting curve); SP04 (21.98 ± 0.45 times shift in clotting curve); and SP05 (12.03 ± 0.12 times shift in clotting curve). These values are independent of relative venom potency, as they reflect the proportional shift of a clotting curve by the antivenom. While there was not a significant statistical correlation between clotting time and antivenom efficacy ($r = 0.820$, $t = 2.024$, $df = 2$, $P = 0.180$), the sample size was $N = 4$, which limited our ability to conclusively demonstrate this effect, despite the high estimated correlation coefficient ($r = 0.82$). Thus, that the boomslang antivenom was able to proportionally shift the clotting curve more for the two more moderately potent venoms (SP02 and SP04) than to the two more potent venoms (SP01 and SP05) is therefore suggestive that the differences in surface chemistry driving clotting activity are key

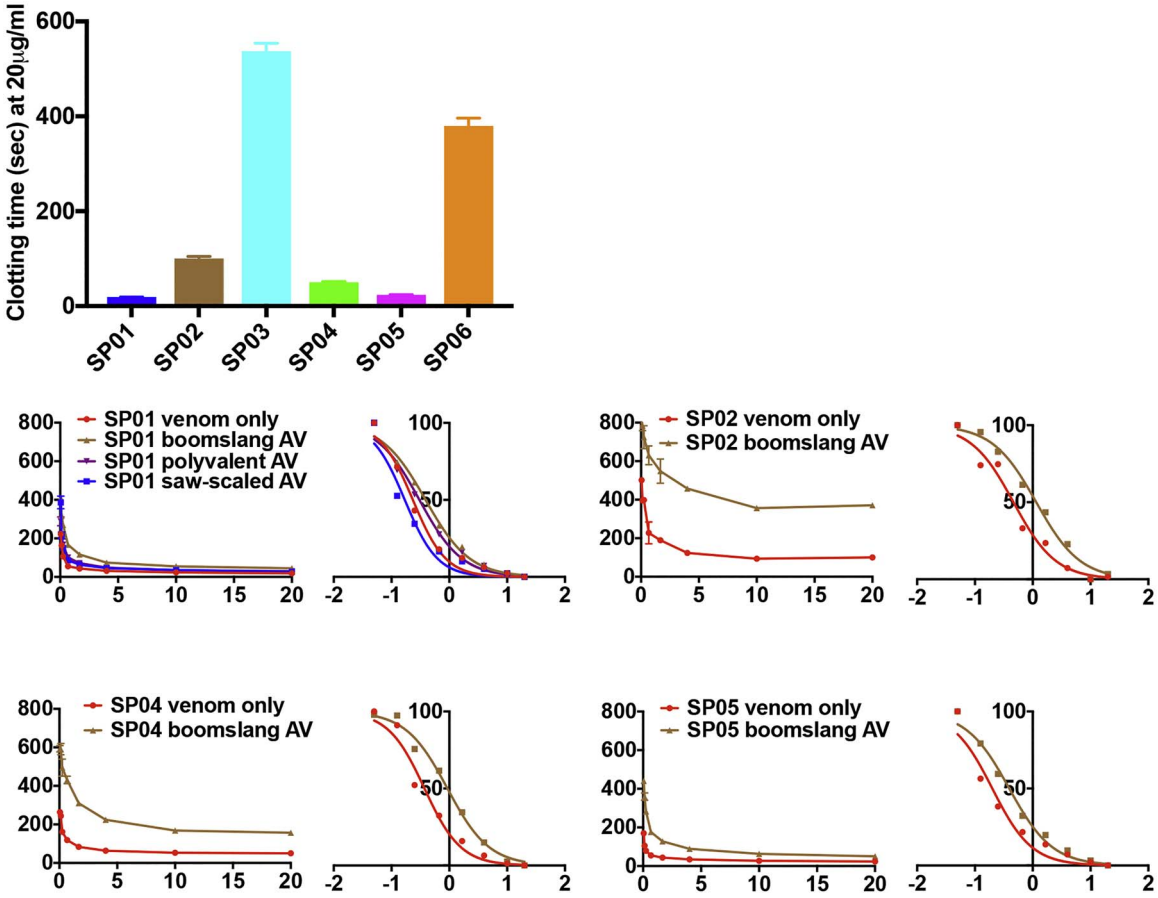

Fig. 1. Clotting times, coagulation dose-response curve and normalised logarithmic transformed views for effects upon recalcified plasma. Red curve lines represent venom in optimal conditions (i.e. with calcium and phospholipid) while other curve colours represent the clotting activity remaining after 2 min preincubation of venom with an antivenom and then the same dilution series were run as for the red line protocol. The antivenom remained a constant in the second protocol while the venom was diluted against it as per the curve graph x-axis concentrations (µg/ml). The curve graph y-axis is time (sec). Normalised logarithmic graph x-axis is log concentration (µg/ml) and y-axis is normalised time (%). Values are means from N = 3. Standard deviation bars are shown for each data point, although for most points the error bars are smaller than the dot point. (For interpretation of the references to color in this figure legend, the reader is referred to the web version of this article.)

sites that also guide relative antivenom efficacy.

3.2. Calibrated automated thromography (CAT)

To evaluate the ability to generate endogenous thrombin in plasma samples, assessment was carried out on a Fluoroskan Ascent fluorometer with the CAT (calibrated automated thrombography) function. The venoms showed significant diversity in the ability to produce thrombin (Fig. 2), with SP01 and SP05 being the most potent. We found a very strong correlation between CAT and clotting time (r = 0.912, t = 4.444, df = 4, P = 0.011).

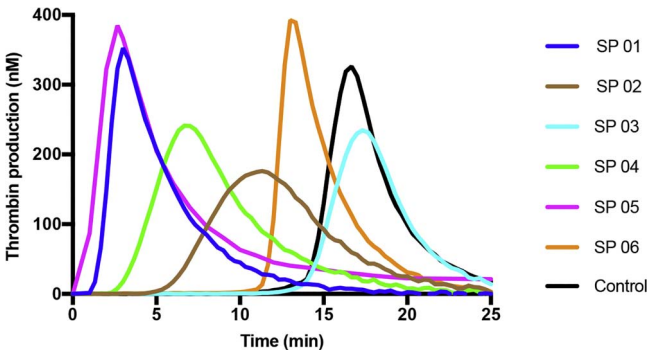

Fig. 2. Calibrated Automated Thrombogram curves for 0.083 µg/ml venom concentration on human plasma. X-axis is time (sec) and y-axis is nM of thrombin production. Values are N = 3.

3.3. Zymogen activation: Factor X and prothrombin

To evaluate the ability to activate the zymogens Factor X and prothrombin, assessment was carried out on a Fluoroskan Ascent fluorometer. Zymogen testing revealed that the clotting action (Fig. 1) and thrombin production (Fig. 2) was not due to activation of prothrombin but was due to the activation of Factor X (Fig. 3). Consistent with the clotting times and CAT patterns, the most potent were SP01, SP04 and SP05. While we were unable to demonstrate a direct correlation

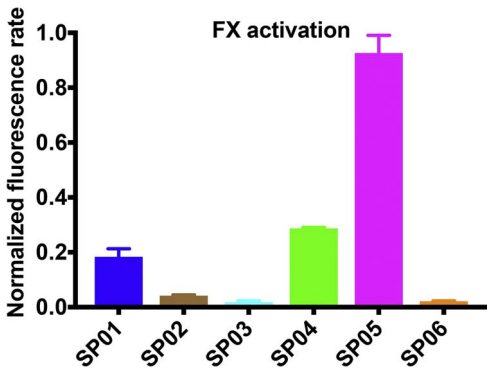

Fig. 3. Relative ability to activate Factor X. Values are N = 3.

between Factor X activation and CAT (r = −0.694, t = −1.931, df = 4, P = 0.126) or Factor X activation and CAT (r = −0.551, t = −1.320, df = 4, P = 0.258), this may be a result of low sample size given the reasonably high estimated correlation coefficient. The correlation coefficient is a negative value because a higher level of Factor X activity would produce quick CAT and clotting times. This discordance between correlation coefficient and other statistical values would have been strongly influenced in the Factor X activation assay by SP05 being disproportionately more potent than SP01 and SP04, in contrast to the clotting and thrombin generation assays where SP01 and SP05 did not vary significantly (Figs. 1 and 2). This variance in relative patterns may be explained by the clotting and thrombin assays being run in plasma and thus additional interactions and dynamics coming into play beyond that of simple Factor X activation as assayed in this test.

3.4. Thromboelastography

To evaluate the strength of plasma clots formed by procoagulant mechanisms, assessment was undertaken using a Thromboelastograph (TEG) viscoelastic hemostatic assay, where strength of the clot is measured as the maximum amplitude of a clotting curve (i.e. thrombus velocity curve) in millimeters. TEG analyses of venom effects upon plasma showed that all venoms were able to form strong, stable clots (Fig. 4A) consistent with their relative plasma clotting times (Fig. 1), CAT effects (Fig. 2) and in line with the ability to activate Factor X (Fig. 3). Relative to the time to spontaneous clotting exhibited by recalcified plasma, the venoms were faster by ratios of: SP01 (21.80), SP02 (3.02), SP03 (1.11), SP04 (8.23), SP05 (12.67), AND SP06 (1.56). Only SP03 did not differ significantly from the control, which was also consistent with the negligible effects upon clotting time (Fig. 1), CAT (Fig. 2) and Factor X activation (Fig. 3) results. TEG plasma testing was strongly and positively correlated with both clotting time (r = 0.983, t = 10.696, df = 4, P = 0.0004) and CAT (r = 0.835, t = 3.040, df = 4, P = 0.038), but in contrast we found no evidence of a correlation between TEG and Factor X activation (r = −0.486, t = −1.028, df = 4, P = 0.362) due to the disproportionate effect SP05 had in the Factor X activation assay.

Thromboelastography analyses of direct effects upon fibrinogen showed that only SP01 and SP05 were also able to cleave fibrinogen to form clots of about 50% the strength of those formed by thrombin (Fig. 4B). None of the other venoms were able to clot or degrade fibrinogen in such a way that thrombin added after 30 min formed other than a normal size and strength clot (Fig. 4C).

3.5. Cleavage of fibrinogen

To quantify the cleavage of the fibrinogen chains (Aα, Bβ and γ), 1D reduced PAGE gels were performed for fibrinogen samples which had been incubated with venom. Extreme diversity between the specimens was evident in the relative speed of cleavage of Aα and Bβ chain cleavage (Fig. 5), with SP05 being the most potent in this regard, but with none of the venoms cleaving the gamma chain. Normalised potency values for the Aα chain cleavage activity were SP01 (0.90 ± 0.2), SP02 (0.171 ± 0.12), SP03 (0.197 ± 0.03), SP04 (0.54 ± 0.02), SP05 (0.99 ± 00.01), and SP06 (0.55 ± 0.01) while normalised potency values for the Bβ chain cleavage activity were SP01 (0.32 ± 0.07), SP02 (0.14 ± 0.09), SP03 (0.08 ± 0.02), SP04 (0.15 ± 0.02), SP05 (0.98 ± 0.02), and SP06 (0.39 ± 0.03). Activity

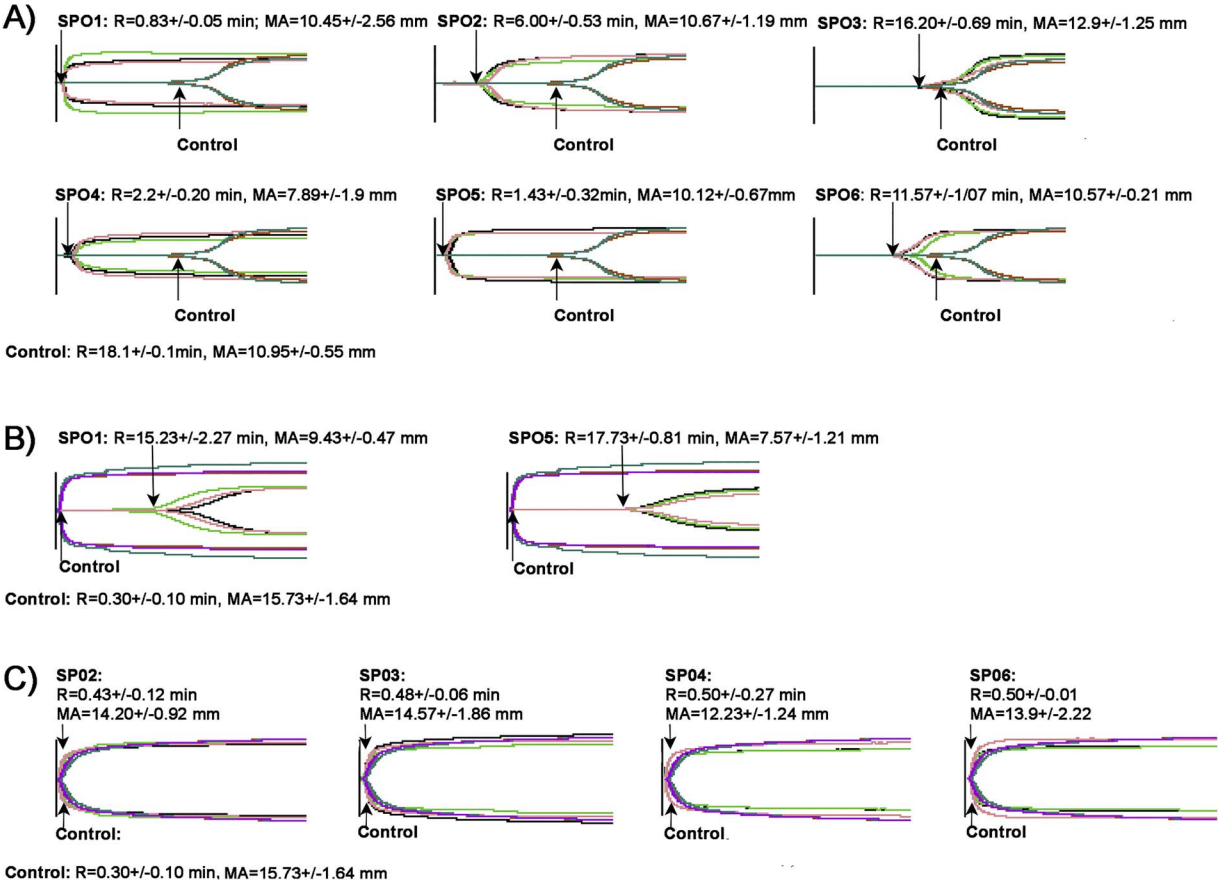

Fig. 4. Overlaid thromboelastography traces showing effects of: A) ability to clot recalcified plasma relative to spontaneous clotting control; B) samples ability to clot fibrinogen relative to thrombin control; and C) thrombin added to samples which did not clot fibrinogen after 30 min in order to test for venom-induced fibrinogen degradation relative to blank control. R = time to initial clot formation. MA (maximum amplitude) = clot strength. Overlaid traces are N = 3 for each set of control or experimental conditions. Values are N = 3 means and standard deviation.

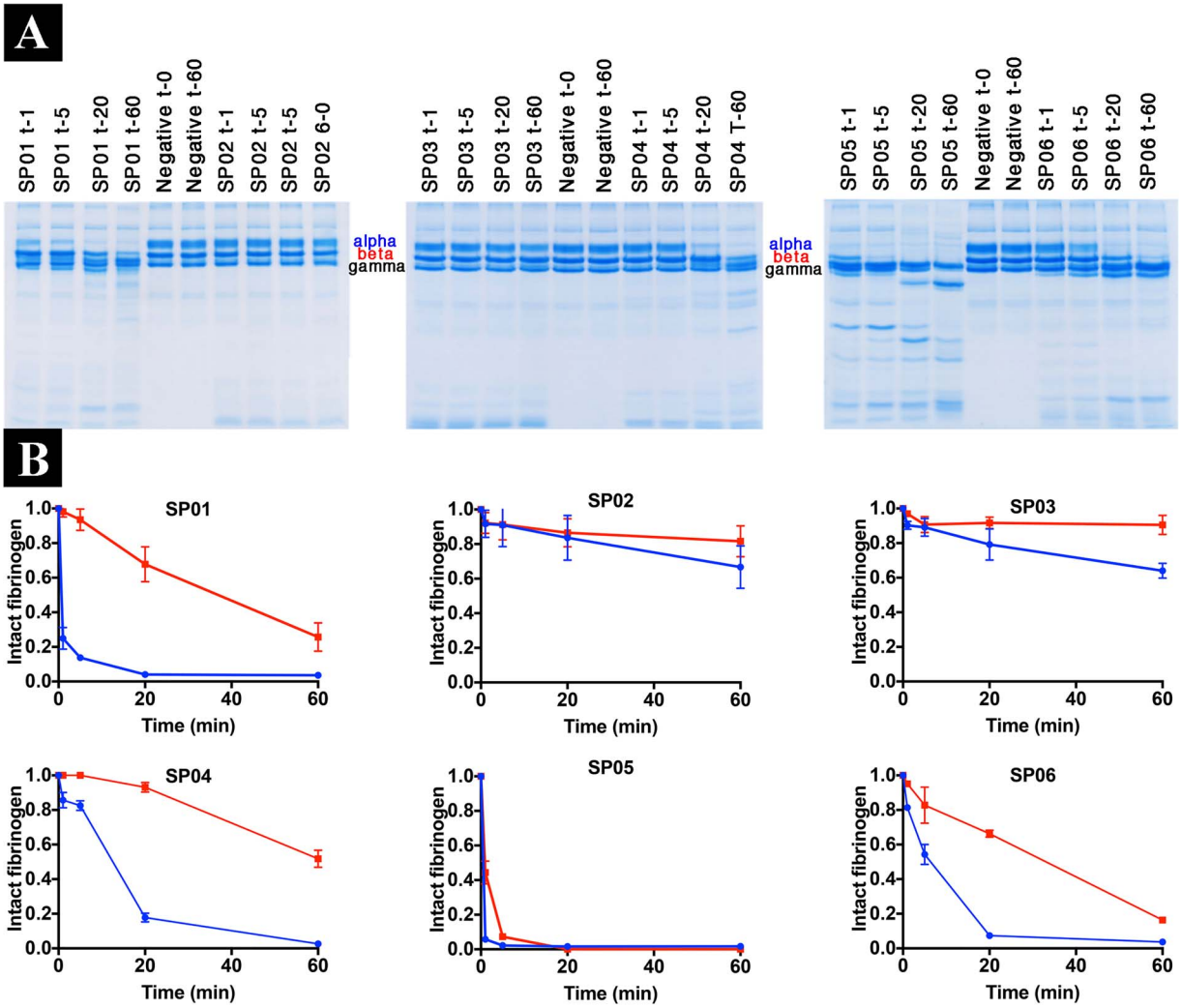

Fig. 5. Differential ability to degrade the alpha, beta and gamma chains of fibrinogen. Experiments were conducted in triplicate. A) Representative 1D-SDS PAGE gel images showing the differential cleavage of fibrinogen over the time periods 1, 5, 20 and 60 min. B) Fibrinogen cleavage visualized as graphing of the change in band density over time. Values are N = 3.

on substrate ES002 was strongly positively correlated with the ability to degrade both the Aα ($r = 0.829$, $t = 2.968$, $df = 4$, $P = 0.041$) and Bβ ($r = 0.807$, $t = 2.731$, $df = 4$, $P = 0.052$) chains of fibrinogen. Note that the correlation is significant for the alpha chain and marginally non-significant in the beta chain, though the latter is likely a consequence of the small sample size as the correlation coefficient is strong ($r > 0.7$). The ability to degrade the alpha and beta chains of fibrinogen was also strongly positively correlated with each other ($r = 0.786$, $t = 2.544$, $df = 4$, $P = 0.064$).

3.6. Cleavage of fluorescent substrates

To assess enzymatic activities, a Fluoroskan Ascent fluorometer and fluorescent substrates known to be cleaved by metalloprotease, serine protease and phospholipase A_2 enzymes were used as proxy indicators for the presence of certain toxin classes. There was a tremendous functional diversity within the venoms (Fig. 6). There was no taxonomical pattern between the species according to enzymatic activity in relation to species designation or confirmed geographical origins.

4. Discussion

The *Atractaspis* venoms displayed the ability to clot plasma (Fig. 1) due to thrombin generation (Fig. 2) as a result of Factor X activation (Fig. 3), resulting in the formation of strong clots in plasma (Fig. 4). The cofactor dependency was absolute in regards to calcium, with all venoms displaying no activity in the absence of calcium, while tests performed in the absence of phospholipid displayed almost half the activity. While SP01 and SP05 were also shown to directly clot fibrinogen (Fig. 4B), the speed of action was much slower than that of the thrombin-generation driven clotting and thus would not be likely to contribute to envenomation effects. The other species neither directly clotted fibrinogen (Fig. 4B) nor degraded it to such an extent that thrombin was not able to form a strong, stable clot from the venom-treated fibrinogen (Fig. 4C). Consistent with this, SP01 and SP05 were most potent in the fibrinogen gel analyses (Fig. 5).

The relative potency of SP01 and SP05 were on par with that of snakes characterized as having lethal levels of thrombin-generation ability such as saw-scaled vipers (*Echis* species) (Rogalski et al., 2017). In addition to risk from bites in the wild, specimens from the *Atractaspis* genus are regularly imported into the exotic pet trade and thus are a source of exotic snakebite in the developed world. Therefore, the potent procoagulant action revealed in this study is cause for concern.

In this study, the ability of available African antivenoms to neutralize the venoms varied, with the SAVP boomslang antivenom being the most relatively effective. While the level of efficacy of the best neutralized species was less than half that of the target species *Dispholidus typus* (Debono et al., 2017), the most potent species were neutralized at a relative level of less than seven times that of *D. typus* efficacy levels and on par with the poorly neutralized *Thelatornis*

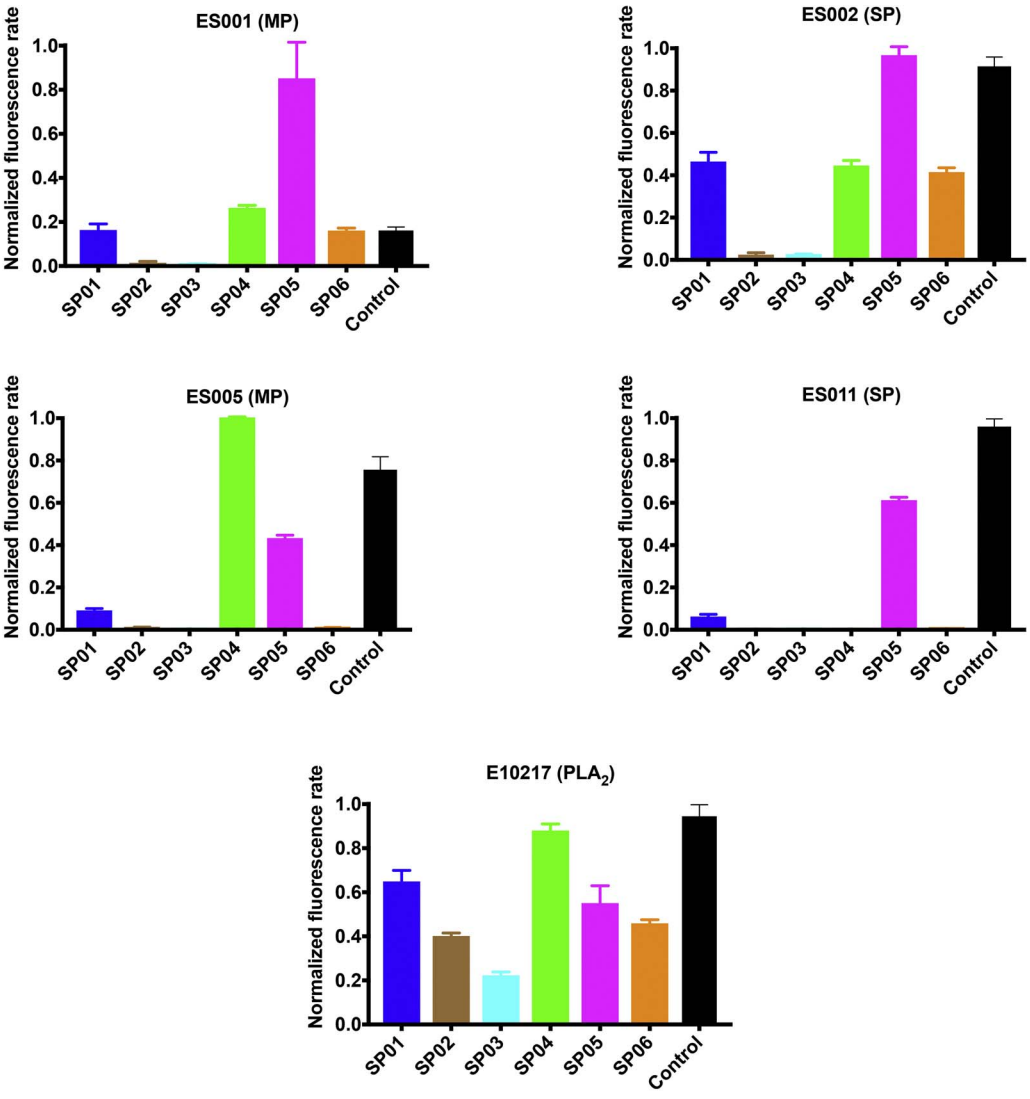

Fig. 6. Relative venom (10 ng/μl) action upon fluorogenic peptide substrates: ES001 (Mca-PLGL-Dpa-AR-NH_2); ES002 (Mca-Arg-Pro-Lys-Pro-Val-Glu-Nval-Trp-Arg-Lys (Dnp)-NH_2); ES005 (Mca-Arg-Pro-Pro-Gly-Phe-Ser-Ala-Phe-Lys(Dnp)-OH); ES011 (Boc-Val-Pro-Arg-AMC. Boc: *t*-Butyloxycarbonyl; 7-Amino-4-methylcoumarin); and E10217 (glycerophospho-ethanolamine with a BODIPY® FL dye-labeled sn-2 acyl chain). Broad enzyme classes known to cleave a particular substrate are shown parenthetically: PLA_2 = phospholipase A_2; MP = metalloprotease; and SP = serine protease. Column values obtained from normalisation of slope values. X axis: species name; Y axis: absorbance percentage. Analysis of triplicates was conducted on GraphPad PRISM 7.0 and error bars indicate standard deviation.

mossambicus (Debono et al., 2017). This suggests that, while the SAVP boomslang antivenom does neutralize the coagulotoxic effects of *Atractaspis* venoms, the efficacy levels indicate that impractical, large amounts of antivenom would be required. In contrast, as the SAVP polyvalent and saw-scaled antivenoms performed comparatively poorly, even under the idealized testing regime in this study, it is very unlikely they would have any significant clinical efficacy.

The protocols used in this study to characterize coagulation effects, cofactor dependency and antivenom efficacy have been previously validated on diverse genera ranging from colubrids (*Dispholidus* and *Thelatornis*) (Debono et al., 2017), elapids (*Hoplocephalus, Notechis, Paroplocephalus* and *Tropidechis*) (Lister et al., 2017) and viperids (*Echis*) (Rogalski et al., 2017). These protocols have been shown to be more precise in characterizing the potency and specificity of the coagulation functions than historical WHO protocols incorporating the MCD (minimum coagulant dose) method (Theakston and Reid, 1983).

Similarly, the antivenom testing protocol utilized in this study provides a more accurate estimation of antivenom neutralization ability than the previous WHO methods. Our new method prioritizes rapid, high-affinity antibody-toxin interactions more reflective of real-world scenarios (Debono et al., 2017; Lister et al., 2017; Rogalski et al., 2017). In contrast, the traditional WHO protocol uses prolonged incubation times and thus may overestimate efficacy (Segura et al., 2010; WHO, 1981, 2010a,b), particularly for coagulotoxic venoms which readily degrade. This was shown by us in our study of *Echis* venoms which showed a much narrower taxonomic spectrum of efficacy for the ICP EchiTab-Plus-ICP antivenom (Rogalski et al., 2017) than that which it had been attributed to through the use of the WHO prolonged-incubation protocol (Segura et al., 2010). Indeed, Vargas et al. (2011) observed significant loss of coagulant ability in *Oxyuranus* venoms incubated for 30 min compared to 3 min.

Thromboelastography in this study was able to discriminate between procoagulant (Fig. 4A) and pseudo-procoagulant (Fig. 4B) effects. This method, and the thromboelastometry modification, are becoming increasingly important in snake venom research for such studies due to the ability to determine clot strength and accurately quantify specific effects upon clotting (Dambisya et al., 1994, 1995; Hiremath et al., 2016; Jackson et al., 2016; Nagel et al., 2014; Nielsen, 2018; Nielsen and Bazzell, 2017; Nielsen and Boyer, 2016; Nielsen et al., 2017a,b, 2016, 2018; Oguiura et al., 2014; Strydom et al., 2016).

Calibrated automated thrombography has also been shown to be useful in determining the ability of venoms to generate thrombin (Isbister et al., 2010; Lister et al., 2017). In this study, the venoms were shown to have similar activity levels (i.e. areas under the curve) but with different initiation times and slopes to peak formation (Fig. 2). The nature of the enzymatic actions responsible for these differences should be the subject of future work.

While it was beyond the scope of this study to determine the specific toxin type responsible for the Factor X activation, the cross-reactivity of the *Atractaspis* venoms with SAVP boomslang antivenom suggests that

metalloprotease toxins are the responsible agents due to the well-characterized nature of boomslang venom as dominated by coagulotoxic P-III type snake venom metalloproteases (SVMP) (Debono et al., 2017; Kamiguti et al., 2000; Pla et al., 2017). Factor X activating SVMP have been previously only ever characterized from *Bothrops*, *Daboia, Echis* and *Macrovipera* viperid venoms (Casewell et al., 2015; Hofmann and Bon, 1987; Kisiel et al., 1976; Siigur et al., 2004; Takeya et al., 1992). All Factor X activating SVMP are coupled to a pair of lectin chains (thus are P-IIId SVMP) and are calcium dependent (Morita, 1998). Factor X activation has also been reported for calcium-dependent kallikrein-type serine proteases from *Bungarus* and *Ophiophagus* elapid venoms and *Cerastes* viperid venoms (Morita, 1998; Vaiyapuri et al., 2015). However, the relative levels or potency of the Factor X activating kallikrein-type serine proteases in *Bungarus, Ophiophagus* and *Cerastes* venoms suggests that they play little, if any, role in prey capture or the development of clinical pathologies in those venoms.

The ability to cleave fibrinogen in a thrombin-like, pseudo-procoagulant manner to form weak, unstable clots (Fig. 4B) is well-characterized in viperid venoms (with some suggestion of this activity also present in elapid venoms such as *Micrurus*) and in viper venoms has been shown to be due to kallikrein-type serine proteases (Vaiyapuri et al., 2015). In contrast, the ability to degrade fibrinogen in a non-clotting manner (Fig. 5) has been widely observed for SVMP in snakes (Casewell et al., 2015) and for kallikrein-type serine proteases in lizard and snake venoms (Hendon and Tu, 1981; Koludarov et al., 2017; Vaiyapuri et al., 2015).

While fibrinogen clotting cleavage has been reported for only kallikrein-type serine proteases, it remains to be elucidated in *Atractaspis* venoms which toxin type is responsible for this function. This should be the subject of future work, just as such efforts should be undertaken to confirm SVMPs are responsible for the Factor X activation activity in these enigmatic and rare venoms. In addition, DNA typing of specimens should be undertaken in order to conclusively link taxonomy with toxinology in these species which are notoriously hard to identify using only external features such as scalation patterns.

In conclusion, this study reveals previously unknown and extreme potent coagulotoxic actions in the *Atractaspis* genus and thus provides information to guide clinicians. Importantly, our results suggest limited management options in treating *Atractaspis* envenomations due to poor antivenom neutralization capacity.

Author contributions

BGF conceived and designed the experiments; BO, JSD, CNZ, CL, FC, BB, JD, AR, and BGF performed the experiments; BO, JSD, CNZ, KA and BGF analyzed the data; AV, RF, and NF contributed reagents/materials/analysis tools; BO, JSD, CNZ, KA, CL, FC, BB, JD, AR, and BGF wrote the paper.

Conflicts of interest

The authors declare no conflict of interest.

Acknowledgment

JSD, CNZ, BB, and JD were supported by University of Queensland Ph.D. scholarships.

References

Abd-Elsalam, M.A., 2011. Bosentan, a selective and more potent antagonist for *Atractaspis* envenomation than the specific antivenom. Toxicon 57, 861–870.

Arlinghaus, F.T., Fry, B.G., Sunagar, K., Jackson, T.N.W., Eble, J.A., Reeks, T., Clemetson, K.J., 2015. Lectin proteins. In: Fry, B.G. (Ed.), Venomous Reptiles and Their Toxins: Evolution, Pathophysiology and Biodiscovery. Oxford University Press, New York, pp. 299–311.

Atkins, A.R., Martin, R.C., Smith, R., 1995. 1H NMR studies of sarafotoxin SRTb, a nonselective endothelin receptor agonist, and IRL 1620, an ETB receptor-specific agonist. Biochemistry 34, 2026–2033.

Borgheresi, R.A., Palma, M.S., Ducancel, F., Camargo, A.C., Carmona, E., 2001. Expression and processing of recombinant sarafotoxins precursor in *Pichia pastoris*. Toxicon 39, 1211–1218.

Boyer, L., Alagón, A., Fry, B.G., Jackson, T.N.W., Sunagar, K., Chippaux, J.P., 2015. Signs, symptoms and treatment of envenomation. In: Fry, B.G. (Ed.), Venomous Reptiles and Their Toxins: Evolution, Pathophysiology and Biodiscovery. Oxford University Press, New York, pp. 32–60.

Casewell, N.R., Sunagar, K., Takacs, Z., Calvete, J.J., Jackson, T.N.W., Fry, B.G., 2015. Snake venom metalloprotease enzymes. In: Fry, B.G. (Ed.), Venomous Reptiles and Their Toxins: Evolution, Pathophysiology and Biodiscovery. Oxford University Press, New York, pp. 347–363.

Cipriani, V., Debono, J., Goldenberg, J., Jackson, T.N.W., Arbuckle, K., Dobson, J., Koludarov, I., Li, B., Hay, C., Dunstan, N., Allen, L., Hendrikx, I., Kwok, H.F., Fry, B.G., 2017. Correlation between ontogenetic dietary shifts and venom variation in Australian brown snakes (*Pseudonaja*). Comp. Biochem. Physiol. Toxicol. Pharmacol.: CBP 197, 53–60.

Clauss, A., 1957. Rapid physiological coagulation method in determination of fibrinogen. Acta Haematol. 17, 237–246.

Coppola, M., Hogan, D.E., 1992. Venomous snakes of southwest Asia. Am. J. Emerg. Med. 10, 230–236.

Dambisya, Y.M., Lee, T.L., Gopalakrishnakone, P., 1994. Action of *Calloselasma rhodostoma* (Malayan pit viper) venom on human blood coagulation and fibrinolysis using computerized thromboelastography (CTEG). Toxicon 32, 1619–1626.

Dambisya, Y.M., Lee, T.L., Gopalakrishnakone, P., 1995. Anticoagulant effects of *Pseudechis australis* (Australian king brown snake) venom on human blood: a computerized thromboelastography study. Toxicon 33, 1378–1382.

Debono, J., Dobson, J., Casewell, N.R., Romilio, A., Li, B., Kurniawan, N., Mardon, K., Weisbecker, V., Nouwens, A., Kwok, H.F., Fry, B.G., 2017. Coagulating colubrids: evolutionary, pathophysiological and biodiscovery implications of venom variations between boomslang (*Dispholidus typus*) and twig snake (*Thelotornis mossambicanus*). Toxins (Basel) 9.

Dobson, J., Yang, D.C., Op den Brouw, B., Cochran, C., Huynh, T., Kurrupu, S., Sanchez, E.E., Massey, D.J., Baumann, K., Jackson, T.N.W., Nouwens, A., Josh, P., Neri-Castro, E., Alagon, A., Hodgson, W.C., Fry, B.G., 2017. Rattling the border wall: pathophysiological implications of functional and proteomic venom variation between Mexican and US subspecies of the desert rattlesnake *Crotalus scutulatus*. Comp. Biochem. Physiol. Toxicol. Pharmacol.: CBP S1532-0456(17)30192-8.

Earl, S., Sunagar, K., Jackson, T.N.W., Fry, B.G., 2015. Factor Va enzymes. In: Fry, B.G. (Ed.), Venomous Reptiles and Their Toxins: Evolution, Pathophysiology and Biodiscovery. Oxford University Press, New York, pp. 255–260.

Eng, W.S., Fry, B.G., Sunagar, K., Takacs, Z., Jackson, T.N.W., Guddat, L.W., 2015. Kunitz peptides. In: Fry, B.G. (Ed.), Venomous Reptiles and Their Toxins: Evolution, Pathophysiology and Biodiscovery. Oxford University Press, New York, pp. 281–290.

Fry, B.G., Sunagar, K., Casewell, N.R., Kochva, E., Roelants, K., Scheib, H., Wüster, W., Vidal, N., Young, B., Burbrink, F., Pyron, R.A., Vonk, F.J., Jackson, T.N.W., 2015. The origin and evolution of the Toxicofera reptile venom system. In: Fry, B.G. (Ed.), Venomous Reptiles and Their Toxins: Evolution, Pathophysiology and Biodiscovery. Oxford University Press, New York, pp. 1–31.

Goyffon, M., 1994. Facts on venomous animals. Ann. Pharm. Fr. 52, 99–109.

Hemker, H.C., Giesen, P., AlDieri, R., Regnault, V., de Smed, E., Wagenvoord, R., Lecompte, T., Beguin, S., 2002. The calibrated automated thrombogram (CAT): a universal routine test for hyper- and hypocoagulability. Pathophysiol. Haemost. Thromb. 32, 249–253.

Hemker, H.C., Giesen, P., Al Dieri, R., Regnault, V., de Smedt, E., Wagenvoord, R., Lecompte, T., Beguin, S., 2003. Calibrated automated thrombin generation measurement in clotting plasma. Pathophysiol. Haemost. Thromb. 33, 4–15.

Hemker, H.C., 2005. Calibrated automated thrombinography (CAT). Thromb. Res. 115, 255.

Hendon, R.A., Tu, A.T., 1981. Biochemical characterization of the lizard toxin gilatoxin. Biochemistry 20, 3517–3522.

Herrera, M., Fernandez, J., Vargas, M., Villalta, M., Segura, A., Leon, G., Angulo, Y., Paiva, O., Matainaho, T., Jensen, S.D., Winkel, K.D., Calvete, J.J., Williams, D.J., Gutierrez, J.M., 2012. Comparative proteomic analysis of the venom of the taipan snake, *Oxyuranus scutellatus*, from Papua New Guinea and Australia: role of neurotoxic and procoagulant effects in venom toxicity. J. Proteom. 75, 2128–2140.

Hiremath, V., Nanjaraj Urs, A.N., Joshi, V., Suvilesh, K.N., Savitha, M.N., Urs Amog, P., Rudresha, G.V., Yariswamy, M., Vishwanath, B.S., 2016. Differential action of medically important Indian BIG FOUR snake venoms on rodent blood coagulation. Toxicon 110, 19–26.

Hofmann, H., Bon, C., 1987. Blood coagulation induced by the venom of *Bothrops atrox*. 2. Identification purification, and properties of two factor X activators. Biochemistry 26, 780–787.

Hutton, R.A., Warrell, D.A., 1993. Action of snake venom components on the haemostatic system. Blood Rev. 7, 176–189.

Isbister, G.K., Woods, D., Alley, S., O'Leary, M.A., Seldon, M., Lincz, L.F., 2010. Endogenous thrombin potential as a novel method for the characterization of procoagulant snake venoms and the efficacy of antivenom. Toxicon 56, 75–85.

Ismail, M., Al-Ahaidib, M.S., Abdoon, N., Abd-Elsalam, M.A., 2007. Preparation of a novel antivenom against *Atractaspis* and *Walterinnesia* venoms. Toxicon 49, 8–18.

Jackson, T.N., Koludarov, I., Ali, S.A., Dobson, J., Zdenek, C.N., Dashevsky, D., Op den Brouw, B., Masci, P.P., Nouwens, A., Josh, P., Goldenberg, J., Cipriani, V., Hay, C., Hendrikx, I., Dunstan, N., Allen, L., Fry, B.G., 2016. Rapid radiations and the race to redundancy: an investigation of the evolution of Australian elapid snake venoms. Toxins (Basel) 8.

Kamiguti, A.S., Theakston, R.D., Sherman, N., Fox, J.W., 2000. Mass spectrophotometric evidence for P-III/P-IV metalloproteinases in the venom of the Boomslang (*Dispholidus typus*). Toxicon 38, 1613–1620.
Kawanabe, Y., Nauli, S.M., 2011. Endothelin. Cell. Mol. Life Sci. 68, 195–203.
Kisiel, W., Hermodson, M.A., Davie, E.W., 1976. Factor X activating enzyme from Russell's viper venom: isolation and characterization. Biochemistry 15, 4901–4906.
Kochva, E., 1998. Venomous snakes of Israel: ecology and snakebite. Public Health Rev. 26, 209–232.
Kolb, E., 1991. Endothelins–properties, formation, mechanism of action and significance. Z. Gesamte Inn. Med. 46, 355–360.
Koludarov, I., Jackson, T.N., Brouw, B.O.D., Dobson, J., Dashevsky, D., Arbuckle, K., Clemente, C.J., Stockdale, E.J., Cochran, C., Debono, J., Stephens, C., Panagides, N., Li, B., Manchadi, M.R., Violette, A., Fourmy, R., Hendrikx, I., Nouwens, A., Clements, J., Martelli, P., Kwok, H.F., Fry, B.G., 2017. Enter the dragon: the dynamic and multifunctional evolution of Anguimorpha lizard venoms. Toxins (Basel) 9.
Kurnik, D., Haviv, Y., Kochva, E., 1999. A snake bite by the Burrowing Asp, Atractaspis engaddensis. Toxicon 37, 223–227.
Lee, S.Y., Lee, C.Y., Chen, Y.M., Kochva, E., 1986. Coronary vasospasm as the primary cause of death due to the venom of the burrowing asp, *Atractaspis engaddensis*. Toxicon 24, 285–291.
Leisewitz, A.L., Blaylock, R.S., Kettner, F., Goodhead, A., Goddard, A., Schoeman, J.P., 2004. The diagnosis and management of snakebite in dogs–a southern African perspective. J. S. Afr. Vet. Assoc. 75, 7–13.
Lister, C., Arbuckle, K., Jackson, T.N.W., Debono, J., Zdenek, C.N., Dashevsky, D., Dunstan, N., Allen, L., Hay, C., Bush, B., Gillett, A., Fry, B.G., 2017. Catch a tiger snake by its tail: differential toxicity, co-factor dependence and antivenom efficacy in a procoagulant clade of Australian venomous snakes. Comp. Biochem. Physiol. Toxicol. Pharmacol.: CBP 202, 39–54.
Mahjoub, Y., Malaquin, S., Mourier, G., Lorne, E., Abou Arab, O., Massy, Z.A., Dupont, H., Ducancel, F., 2015. Short- versus long-sarafotoxins: two structurally related snake toxins with very different in vivo haemodynamic effects. PLoS One 10, e0132864.
Malaquin, S., Bayat, S., Abou Arab, O., Mourier, G., Lorne, E., Kamel, S., Dupont, H., Ducancel, F., Mahjoub, Y., 2016. Respiratory effects of sarafotoxins from the venom of different *Atractaspis* genus snake species. Toxins (Basel) 8.
Morita, T., 1998. Proteases which activate factor X. In: Bailey, G.S. (Ed.), Enzymes from Snake Venom. Alaken Inc, Fort Collins, CO, USA, pp. 179–208.
Nagel, S.S., Schoeman, J.P., Thompson, P.N., Wiinberg, B., Goddard, A., 2014. Hemostatic analysis of dogs naturally envenomed by the African puff adder (*Bitis arietans*) and snouted cobra (*Naja annulifera*). J. Vet. Emerg. Crit. Care (San Antonio) 24, 662–671.
Nakajima, K., Kubo, S., Kumagaye, S., Nishio, H., Tsunemi, M., Inui, T., Kuroda, H., Chino, N., Watanabe, T.X., Kimura, T., et al., 1989. Structure-activity relationship of endothelin: importance of charged groups. Biochem. Biophys. Res. Commun. 163, 424–429.
Nayler, W.G., Gu, X.H., Casley, D.J., 1989. Sarafotoxin S6c is a relatively weak displacer of specifically bound 125I-endothelin. Biochem. Biophys. Res. Commun. 161, 89–94.
Nielsen, V.G., Bazzell, C.M., 2017. Carbon monoxide releasing molecule-2 inhibition of snake venom thrombin-like activity: novel biochemical brake. J. Thromb. Thrombolysis 43, 203–208.
Nielsen, V.G., Boyer, L.V., 2016. Iron and carbon monoxide attenuate degradation of plasmatic coagulation by *Crotalus atrox* venom. Blood Coagul. Fibrinolysis 27, 506–510.
Nielsen, V.G., Redford, D.T., Boyle, P.K., 2016. Effect of iron and carbon monoxide on fibrinogenase-like degradation of plasmatic coagulation by venoms of six *Agkistrodon* species. Basic Clin. Pharmacol. Toxicol. 118, 390–395.
Nielsen, V.G., Boyer, L.V., Redford, D.T., Ford, P., 2017a. Thrombelastographic characterization of the thrombin-like activity of *Crotalus simus* and *Bothrops asper* venoms. Blood Coagul. Fibrinolysis 28, 211–217.
Nielsen, V.G., Redford, D.T., Boyle, P.K., 2017b. Effect of iron and carbon monoxide on fibrinogenase-like degradation of plasmatic coagulation by venoms of four *Crotalus* species. Blood Coagul. Fibrinolysis 28, 34–39.
Nielsen, V.G., Sanchez, E.E., Redford, D.T., 2018. Characterization of the rabbit as an in vitro and in vivo model to assess the effects of fibrinogenolytic activity of snake venom on coagulation. Basic Clin. Pharmacol. Toxicol. 122, 157–164.
Nielsen, V.G., 2018. *Crotalus atrox* venom exposed to carbon monoxide has decreased fibrinogenolytic activity *in vivo* in rabbits. Basic Clin. Pharmacol. Toxicol. 122, 82–86.
Oguiura, N., Kapronezai, J., Ribeiro, T., Rocha, M.M., Medeiros, C.R., Marcelino, J.R., Prezoto, B.C., 2014. An alternative micromethod to access the procoagulant activity of *Bothrops jararaca* venom and the efficacy of antivenom. Toxicon 90, 148–154.
Ovadia, M., 1987. Isolation and characterization of a hemorrhagic factor from the venom of the snake *Atractaspis engaddensis* (Atractaspididae). Toxicon 25, 621–630.
Patocka, J., Merka, V., Hrdina, V., Hrdina, R., 2004. Endothelins and sarafotoxins: peptides of similar structure and different function. Acta Med. (Hradec Kralove) 47, 157–162.
Pla, D., Sanz, L., Whiteley, G., Wagstaff, S.C., Harrison, R.A., Casewell, N.R., Calvete, J.J., 2017. What killed Karl Patterson Schmidt? Combined venom gland transcriptomic, venomic and antivenomic analysis of the South African green tree snake (the boomslang), *Dispholidus typus*. Biochim. Biophys. Acta 1861, 814–823.
Rogalski, A., Soerensen, C., Op den Brouw, B., Lister, C., Dashevsky, D., Arbuckle, K., Gloria, A., Zdenek, C.N., Casewell, N.R., Gutierrez, J.M., Wuster, W., Ali, S.A., Masci, P., Rowley, P., Frank, N., Fry, B.G., 2017. Differential procoagulant effects of saw-scaled viper (Serpentes: Viperidae: *Echis*) snake venoms on human plasma and the narrow taxonomic ranges of antivenom efficacies. Toxicol. Lett. 280, 159–170.
Segura, A., Villalta, M., Herrera, M., Leon, G., Harrison, R., Durfa, N., Nasidi, A., Calvete, J.J., Theakston, R.D., Warrell, D.A., Gutierrez, J.M., 2010. Preclinical assessment of the efficacy of a new antivenom (EchiTAb-Plus-ICP) for the treatment of viper envenoming in sub-Saharan Africa. Toxicon 55, 369–374.
Siigur, E., Aaspollu, A., Trummal, K., Tonismagi, K., Tammiste, I., Kalkkinen, N., Siigur, J., 2004. Factor X activator from *Vipera lebetina* venom is synthesized from different genes. Biochim. Biophys. Acta 1702, 41–51.
Spawls, S., Branch, B., 1995. Dangerous Snakes of Africa. Blandford Press, London, UK.
Strydom, M.A., Bester, J., Mbotwe, S., Pretorius, E., 2016. The effect of physiological levels of South African puff adder (*Bitis arietans*) snake venom on blood cells: an in vitro model. Sci. Rep. 6, 35988.
Sunagar, K., Jackson, T.N.W., Reeks, T., Fry, B.G., 2015a. Group I phospholipase A2 enzymes. In: Fry, B.G. (Ed.), Venomous Reptiles and Their Toxins: Evolution, Pathophysiology and Biodiscovery. Oxford University Press, New York pp. 327-324.
Sunagar, K., Tsai, I.H., Lomonte, B., Jackson, T.N.W., Fry, B.G., 2015b. Group II phospholipase A_2 enzymes. In: Fry, B.G. (Ed.), Venomous Reptiles and Their Toxins: Evolution, Pathophysiology and Biodiscovery. Oxford University Press, New York, pp. 335–340.
Takasaki, C., Itoh, Y., Onda, H., Fujino, M., 1992. Cloning and sequence analysis of a snake, *Atractaspis engaddensis* gene encoding sarafotoxin S6c. Biochem. Biophys. Res. Commun. 189, 1527–1533.
Takeya, H., Nishida, S., Miyata, T., Kawada, S., Saisaka, Y., Morita, T., Iwanaga, S., 1992. Coagulation factor X activating enzyme from Russell's viper venom (RVV-X): a novel metalloproteinase with disintegrin (platelet aggregation inhibitor)-like and C-type lectin-like domains. J. Biol. Chem. 267, 14109–14117.
Terrat, Y., Sunagar, K., Fry, B.G., Jackson, T.N., Scheib, H., Fourmy, R., Verdenaud, M., Blanchet, G., Antunes, A., Ducancel, F., 2013. *Atractaspis aterrima* toxins: the first insight into the molecular evolution of venom in side-stabbers. Toxins (Basel) 5, 1948–1964.
Theakston, R.D., Reid, H.A., 1983. Development of simple standard assay procedures for the characterization of snake venom. Bull. World Health Organ. 61, 949–956.
Tilbury, C.R., Verster, J., 2016. A fatal bite from the burrowing asp *Atractaspis corpulenta* (Hallowell 1854). Toxicon 118, 21–26.
Trabi, M., Sunagar, K., Jackson, T.N.W., Fry, B.G., 2015. Factor Xa enzymes. In: Fry, B.G. (Ed.), Venomous Reptiles and Their Toxins: Evolution, Pathophysiology and Biodiscovery. Oxford University Press, New York, pp. 261–266.
Utkin, Y., Sunagar, K., Jackson, T.N.W., Reeks, T., Fry, B.G., 2015. Three-finger toxins (3FTxs). In: Fry, B.G. (Ed.), Venomous Reptiles and Their Toxins: Evolution, Pathophysiology and Biodiscovery. Oxford University Press, New York, pp. 215–227.
Vaiyapuri, S., Sunagar, K., Gibbins, J.M., Jackson, T.N.W., Reeks, T., Fry, B.G., 2015. Kallikrein enzymes. In: Fry, B.G. (Ed.), Venomous Reptiles and Their Toxins: Evolution, Pathophysiology and Biodiscovery. Oxford University Press, New York, pp. 267–280.
Vargas, M., Segura, A., Herrera, M., Villalta, M., Estrada, R., Cerdas, M., Paiva, O., Matainaho, T., Jensen, S.D., Winkel, K.D., León, G., Gutiérrez, J.M., Williams, D.J., 2011. Preclinical evaluation of caprylic acid-fractionated IgG antivenom for the treatment of Taipan (*Oxyuranus scutellatus*) envenoming in Papua New Guinea. PLoS Negl. Trop. Dis. 5 (5), e1144.
Warrell, D.A., Ormerod, L.D., Davidson, N.M., 1976. Bites by the night adder (*Causus maculatus*) and burrowing vipers (genus *Atractaspis*) in Nigeria. Am. J. Trop. Med. Hyg. 25, 517–524.
WHO, 1981. Progress in the Characterization of Venoms and Standardization of Antivenoms. World Health Organization, Geneva.
WHO, 2010a. Guidelines for the Prevention and Clinical Management of Snakebite in Africa. WHO, Geneva.
WHO, (Ed.), 2010. WHO Guidelines for the Production, Control and Regulation of Snake Antivenom Immunoglobulins, 1–34.